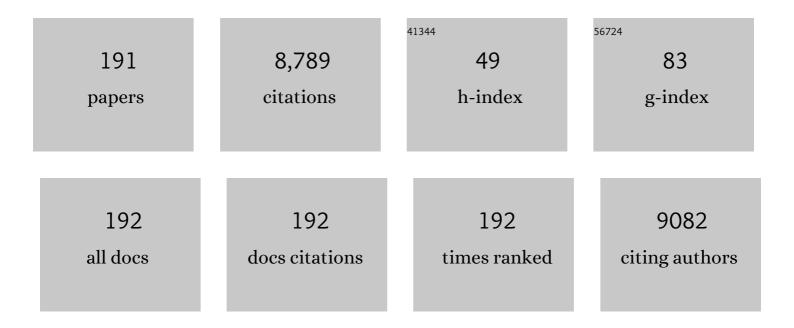
List of Publications by Year in descending order

Source: https://exaly.com/author-pdf/2592054/publications.pdf Version: 2024-02-01



Ιυν Ηου

#	Article	IF	CITATIONS
1	Distinct community structure and microbial functions of biofilms colonizing microplastics. Science of the Total Environment, 2019, 650, 2395-2402.	8.0	387
2	Kinetics and thermodynamics of adsorption of methylene blue by a magnetic graphene-carbon nanotube composite. Applied Surface Science, 2014, 290, 116-124.	6.1	292
3	Iodideâ€Induced Fragmentation of Polymerized Hydrophilic Carbon Nitride for Highâ€Performance Quasiâ€Homogeneous Photocatalytic H ₂ O ₂ Production. Angewandte Chemie - International Edition, 2021, 60, 25546-25550.	13.8	251
4	Synthesis of novel 2D-2D p-n heterojunction BiOBr/La 2 Ti 2 O 7 composite photocatalyst with enhanced photocatalytic performance under both UV and visible light irradiation. Applied Catalysis B: Environmental, 2016, 194, 157-168.	20.2	245
5	Investigation on the adsorption and desorption behaviors of antibiotics by degradable MPs with or without UV ageing process. Journal of Hazardous Materials, 2021, 401, 123363.	12.4	211
6	Significantly enhanced visible light photocatalytic efficiency of phosphorus doped TiO2 with surface oxygen vacancies for ciprofloxacin degradation: Synergistic effect and intermediates analysis. Journal of Hazardous Materials, 2018, 351, 196-205.	12.4	204
7	The effect of excess Zn on mineral nutrition and antioxidative response in rapeseed seedlings. Chemosphere, 2009, 75, 1468-1476.	8.2	198
8	Visible light activated photocatalytic degradation of tetracycline by a magnetically separable composite photocatalyst: Graphene oxide/magnetite/cerium-doped titania. Journal of Colloid and Interface Science, 2016, 467, 129-139.	9.4	186
9	Metabolic adaptations to ammonia-induced oxidative stress in leaves of the submerged macrophyte Vallisneria natans (Lour.) Hara. Aquatic Toxicology, 2008, 87, 88-98.	4.0	149
10	Insights into the short-term effects of CeO2 nanoparticles on sludge dewatering and related mechanism. Water Research, 2017, 118, 93-103.	11.3	142
11	Photocatalytic degradation of tetrabromobisphenol A by a magnetically separable graphene–TiO2 composite photocatalyst: Mechanism and intermediates analysis. Chemical Engineering Journal, 2015, 264, 113-124.	12.7	140
12	Effect of CuO nanoparticles on the production and composition of extracellular polymeric substances and physicochemical stability of activated sludge flocs. Bioresource Technology, 2015, 176, 65-70.	9.6	134
13	Effect of oxygen vacancy on enhanced photocatalytic activity of reduced ZnO nanorod arrays. Applied Surface Science, 2015, 325, 112-116.	6.1	130
14	A one-pot method for the preparation of graphene–Bi2MoO6 hybrid photocatalysts that are responsive to visible-light and have excellent photocatalytic activity in the degradation of organic pollutants. Carbon, 2012, 50, 5256-5264.	10.3	125
15	Combining Heterojunction Engineering with Surface Cocatalyst Modification To Synergistically Enhance the Photocatalytic Hydrogen Evolution Performance of Cadmium Sulfide Nanorods. ACS Sustainable Chemistry and Engineering, 2017, 5, 7670-7677.	6.7	123
16	Noble-metal-free nickel phosphide modified CdS/C ₃ N ₄ nanorods for dramatically enhanced photocatalytic hydrogen evolution under visible light irradiation. Dalton Transactions, 2017, 46, 13793-13801.	3.3	122
17	Phosphate group grafted twinned BiPO4 with significantly enhanced photocatalytic activity: Synergistic effect of improved charge separation efficiency and redox ability. Applied Catalysis B: Environmental, 2018, 234, 90-99.	20.2	115
18	Effects of CeO2 nanoparticles on production and physicochemical characteristics of extracellular polymeric substances in biofilms in sequencing batch biofilm reactor. Bioresource Technology, 2015, 194, 91-98.	9.6	103

#	Article	IF	CITATIONS
19	Acute effects of nanoplastics and microplastics on periphytic biofilms depending on particle size, concentration and surface modification. Environmental Pollution, 2019, 255, 113300.	7.5	100
20	Effects of Pb stress on nutrient uptake and secondary metabolism in submerged macrophyte Vallisneria natans. Ecotoxicology and Environmental Safety, 2011, 74, 1297-1303.	6.0	96
21	Inhibitory effects of ZnO nanoparticles on aerobic wastewater biofilms from oxygen concentration profiles determined by microelectrodes. Journal of Hazardous Materials, 2014, 276, 164-170.	12.4	95
22	Preparation of graphene–carbon nanotube–TiO2 composites with enhanced photocatalytic activity for the removal of dye and Cr (VI). Applied Catalysis A: General, 2014, 473, 83-89.	4.3	95
23	Salicylic acid involved in the regulation of nutrient elements uptake and oxidative stress in Vallisneria natans (Lour.) Hara under Pb stress. Chemosphere, 2011, 84, 136-142.	8.2	94
24	Distribution of metals in water and suspended particulate matter during the resuspension processes in Taihu Lake sediment, China. Quaternary International, 2013, 286, 94-102.	1.5	94
25	Interactions between vegetation, water flow and sediment transport: A review. Journal of Hydrodynamics, 2015, 27, 24-37.	3.2	92
26	Fabrication of novel p–n heterojunction BiOI/La ₂ Ti ₂ O ₇ composite photocatalytic performance under visible light irradiation. Dalton Transactions, 2016, 45, 7986-7997.	3.3	88
27	Effects of biofilm colonization on the sinking of microplastics in three freshwater environments. Journal of Hazardous Materials, 2021, 413, 125370.	12.4	88
28	Preparation, characterization, photocatalytic properties of titania hollow sphere doped with cerium. Journal of Hazardous Materials, 2010, 178, 517-521.	12.4	85
29	Effects of Ag and Ag2S nanoparticles on denitrification in sediments. Water Research, 2018, 137, 28-36.	11.3	84
30	Adsorption and desorption behaviors of antibiotics by tire wear particles and polyethylene microplastics with or without aging processes. Science of the Total Environment, 2021, 771, 145451.	8.0	82
31	Distinct microbial metabolic activities of biofilms colonizing microplastics in three freshwater ecosystems. Journal of Hazardous Materials, 2021, 403, 123577.	12.4	81
32	Preparation of graphene oxide–Ag3PO4 composite photocatalyst with high visible light photocatalytic activity. Applied Surface Science, 2013, 271, 265-270.	6.1	76
33	Response of wastewater biofilm to CuO nanoparticle exposure in terms of extracellular polymeric substances and microbial community structure. Science of the Total Environment, 2017, 579, 588-597.	8.0	76
34	Degradation of Tetrabromobisphenol A by Sulfidated Nanoscale Zerovalent Iron in a Dynamic Two-Step Anoxic/Oxic Process. Environmental Science & Technology, 2019, 53, 8105-8114.	10.0	75
35	Sediment resuspension under action of wind in Taihu Lake, China. International Journal of Sediment Research, 2015, 30, 48-62.	3.5	71
36	Effects of Ag NPs on denitrification in suspended sediments via inhibiting microbial electron behaviors. Water Research, 2020, 171, 115436.	11.3	71

#	Article	IF	CITATIONS
37	<i>In situ</i> surface engineering of ultrafine Ni ₂ P nanoparticles on cadmium sulfide for robust hydrogen evolution. Catalysis Science and Technology, 2018, 8, 5406-5415.	4.1	69
38	Preparation, characterization and photocatalytic activity of the neodymium-doped TiO2 hollow spheres. Applied Surface Science, 2010, 257, 227-231.	6.1	68
39	Effects of CeO2 nanoparticles on biological nitrogen removal in a sequencing batch biofilm reactor and mechanism of toxicity. Bioresource Technology, 2015, 191, 73-78.	9.6	68
40	Excess Zn alters the nutrient uptake and induces the antioxidative responses in submerged plant Hydrilla verticillata (L.f.) Royle. Chemosphere, 2009, 76, 938-945.	8.2	65
41	Algal growth and utilization of phosphorus studied by combined mono-culture and co-culture experiments. Environmental Pollution, 2017, 220, 274-285.	7.5	64
42	Responses of wastewater biofilms to chronic CeO2 nanoparticles exposure: Structural, physicochemical and microbial properties and potential mechanism. Water Research, 2018, 133, 208-217.	11.3	64
43	Enhanced photoelectrocatalytic activity for dye degradation by graphene–titania composite film electrodes. Journal of Hazardous Materials, 2012, 223-224, 79-83.	12.4	63
44	Chlorpyrifos and 3,5,6-trichloro-2-pyridinol degradation in zero valent iron coupled anaerobic system: Performances and mechanisms. Chemical Engineering Journal, 2018, 353, 254-263.	12.7	63
45	Graphene and TiO2 co-modified flower-like Bi2O2CO3: A novel multi-heterojunction photocatalyst with enhanced photocatalytic activity. Applied Surface Science, 2015, 355, 411-418.	6.1	61
46	Transport behavior of micro polyethylene particles in saturated quartz sand: Impacts of input concentration and physicochemical factors. Environmental Pollution, 2020, 263, 114499.	7.5	61
47	Preparation of CdS nanoparticle loaded flower-like Bi ₂ O ₂ CO ₃ heterojunction photocatalysts with enhanced visible light photocatalytic activity. Dalton Transactions, 2015, 44, 11321-11330.	3.3	60
48	Microbial carbon metabolic functions of biofilms on plastic debris influenced by the substrate types and environmental factors. Environment International, 2020, 143, 106007.	10.0	57
49	Enhanced stability and dissolution of CuO nanoparticles by extracellular polymeric substances in aqueous environment. Journal of Nanoparticle Research, 2015, 17, 1.	1.9	53
50	Antioxidant enzyme activities as biomarkers of fluvial biofilm to ZnO NPs ecotoxicity and the Integrated Biomarker Responses (IBR) assessment. Ecotoxicology and Environmental Safety, 2016, 133, 10-17.	6.0	51
51	Assessment of mobilization of labile phosphorus and iron across sediment-water interface in a shallow lake (Hongze) based on in situ high-resolution measurement. Environmental Pollution, 2016, 219, 873-882.	7.5	50
52	Aggregation and removal of copper oxide (CuO) nanoparticles in wastewater environment and their effects on the microbial activities of wastewater biofilms. Bioresource Technology, 2016, 216, 537-544.	9.6	49
53	Effects of CeO2, CuO, and ZnO nanoparticles on physiological features of Microcystis aeruginosa and the production and composition of extracellular polymeric substances. Environmental Science and Pollution Research, 2017, 24, 226-235.	5.3	49
54	Construction of silver iodide/silver/bismuth tantalate Z-scheme photocatalyst for effective visible light degradation of organic pollutants. Journal of Colloid and Interface Science, 2018, 532, 190-200.	9.4	49

#	Article	IF	CITATIONS
55	Preparation of cerium and nitrogen co-doped titania hollow spheres with enhanced visible light photocatalytic performance. Powder Technology, 2011, 210, 203-207.	4.2	47
56	Nanoparticle tracking analysis versus dynamic light scattering: Case study on the effect of Ca2+ and alginate on the aggregation of cerium oxide nanoparticles. Journal of Hazardous Materials, 2018, 360, 319-328.	12.4	47
57	Effect of alginate on the aggregation kinetics of copper oxide nanoparticles (CuO NPs): bridging interaction and hetero-aggregation induced by Ca2+. Environmental Science and Pollution Research, 2016, 23, 11611-11619.	5.3	46
58	Application of zero valent iron coupling with biological process for wastewater treatment: a review. Reviews in Environmental Science and Biotechnology, 2017, 16, 667-693.	8.1	45
59	Investigation on the adsorption and desorption behaviors of heavy metals by tire wear particles with or without UV ageing processes. Environmental Research, 2021, 195, 110858.	7.5	45
60	Bismuth oxychloride modified titanium phosphate nanoplates: A new p-n type heterostructured photocatalyst with high activity for the degradation of different kinds of organic pollutants. Journal of Colloid and Interface Science, 2016, 476, 71-78.	9.4	44
61	Preparation, characterization and photocatalytic activity of a novel composite photocatalyst: Ceria-coated activated carbon. Journal of Hazardous Materials, 2010, 184, 1-5.	12.4	43
62	Investigation on graphene and Pt co-modified CdS nanowires with enhanced photocatalytic hydrogen evolution activity under visible light irradiation. Dalton Transactions, 2015, 44, 16372-16382.	3.3	43
63	In-situ growth of Ag3VO4 nanoparticles onto BiOCI nanosheet to form a heterojunction photocatalyst with enhanced performance under visible light irradiation. Journal of Alloys and Compounds, 2016, 688, 1-7.	5.5	43
64	Effect of UV irradiation on the aggregation of TiO2 in an aquatic environment: Influence of humic acid and pH. Environmental Pollution, 2016, 212, 178-187.	7.5	43
65	Shift in bacterioplankton diversity and structure: Influence of anthropogenic disturbances along the Yarlung Tsangpo River on the Tibetan Plateau, China. Scientific Reports, 2017, 7, 12529.	3.3	43
66	Photoelectrocatalytic determination of chemical oxygen demand under visible light using Cu2O-loaded TiO2 nanotube arrays electrode. Sensors and Actuators B: Chemical, 2013, 181, 1-8.	7.8	42
67	Enhanced photocatalytic properties of the 3D flower-like Mg-Al layered double hydroxides decorated with Ag 2 CO 3 under visible light illumination. Materials Research Bulletin, 2016, 80, 23-29.	5.2	41
68	Effects of ZnO nanoparticles and Zn2+ on fluvial biofilms and the related toxicity mechanisms. Science of the Total Environment, 2016, 544, 230-237.	8.0	41
69	Adsorption of perfluorooctane sulfonate on soils: Effects of soil characteristics and phosphate competition. Chemosphere, 2017, 168, 1383-1388.	8.2	41
70	Aggregation, sedimentation, and dissolution of CuO and ZnO nanoparticles in five waters. Environmental Science and Pollution Research, 2018, 25, 31240-31249.	5.3	41
71	The effect of flow velocity on the distribution and composition of extracellular polymeric substances in biofilms and the detachment mechanism of biofilms. Water Science and Technology, 2014, 69, 825-832.	2.5	40
72	Effects of titanium dioxide nanoparticles on algal and bacterial communities in periphytic biofilms. Environmental Pollution, 2019, 251, 407-414.	7.5	39

#	Article	IF	CITATIONS
73	Effects of iron on growth, antioxidant enzyme activity, bound extracellular polymeric substances and microcystin production of Microcystis aeruginosa FACHB-905. Ecotoxicology and Environmental Safety, 2016, 132, 231-239.	6.0	37
74	Effects of zero valent iron on nitrate removal in anaerobic bioreactor with various carbon-to-nitrate ratios: Bio-electrochemical properties, energy regulation strategies and biological response mechanisms. Chemical Engineering Journal, 2021, 419, 129646.	12.7	37
75	Construction of a composite photocatalyst with significantly enhanced photocatalytic performance through combination of homo-junction with hetero-junction. Catalysis Science and Technology, 2018, 8, 486-498.	4.1	36
76	Low concentrations of copper oxide nanoparticles alter microbial community structure and function of sediment biofilms. Science of the Total Environment, 2019, 653, 705-713.	8.0	36
77	Zero valent iron supported biological denitrification for farmland drainage treatments with low organic carbon: Performance and potential mechanisms. Science of the Total Environment, 2019, 689, 1044-1053.	8.0	35
78	Adsorption behavior of lead on aquatic sediments contaminated with cerium dioxide nanoparticles. Environmental Pollution, 2016, 219, 416-424.	7.5	34
79	Effects of CeO 2 nanoparticles on sludge aggregation and the role of extracellular polymeric substances – Explanation based on extended DLVO. Environmental Research, 2016, 151, 698-705.	7.5	34
80	Transport, retention, and long-term release behavior of polymer-coated silver nanoparticles in saturated quartz sand: TheÂimpact of natural organic matters and electrolyte. Environmental Pollution, 2017, 229, 49-59.	7.5	34
81	The effect of anthropogenic impoundment on dissolved organic matter characteristics and copper binding affinity: Insights from fluorescence spectroscopy. Chemosphere, 2017, 188, 424-433.	8.2	34
82	Antibiotic resistance genes attenuation in anaerobic microorganisms during iron uptake from zero valent iron: An iron-dependent form of homeostasis and roles as regulators. Water Research, 2021, 195, 116979.	11.3	34
83	Effects of Nanoplastics on Freshwater Biofilm Microbial Metabolic Functions as Determined by BIOLOG ECO Microplates. International Journal of Environmental Research and Public Health, 2019, 16, 4639.	2.6	33
84	The effect of carbonization temperature on the capacity and mechanisms of Pb(II) adsorption by microalgae residue-derived biochar. Ecotoxicology and Environmental Safety, 2021, 225, 112750.	6.0	33
85	Effect of TiO2 and CeO2 nanoparticles on the metabolic activity of surficial sediment microbial communities based on oxygen microelectrodes and high-throughput sequencing. Water Research, 2018, 129, 287-296.	11.3	32
86	Effects of silver nanoparticles on coupled nitrification–denitrification in suspended sediments. Journal of Hazardous Materials, 2020, 389, 122130.	12.4	32
87	Modeling the Effects of Hydrodynamic Regimes on Microbial Communities within Fluvial Biofilms: Combining Deterministic and Stochastic Processes. Environmental Science & Technology, 2015, 49, 12869-12878.	10.0	31
88	Fabrication of p-type BiOCl/n-type La ₂ Ti ₂ O ₇ facet-coupling heterostructure with enhanced photocatalytic performance. RSC Advances, 2016, 6, 48599-48609.	3.6	31
89	The use of zero-valent iron (ZVI)–microbe technology for wastewater treatment with special attention to the factors influencing performance: A critical review. Critical Reviews in Environmental Science and Technology, 2017, 47, 877-907.	12.8	31
90	Co-adsorption of perfluorooctane sulfonate and phosphate on boehmite: Influence of temperature, phosphate initial concentration and pH. Ecotoxicology and Environmental Safety, 2017, 137, 71-77.	6.0	31

#	Article	IF	CITATIONS
91	The sustainability of riceâ€erayfish coculture systems: a mini review of evidence from Jianghan plain in China. Journal of the Science of Food and Agriculture, 2021, 101, 3843-3853.	3.5	31
92	Modeling of sediment and heavy metal transport in Taihu Lake, China. Journal of Hydrodynamics, 2013, 25, 379-387.	3.2	30
93	Modeling the Biodegradation of Bacterial Community Assembly Linked Antibiotics in River Sediment Using a Deterministic–Stochastic Combined Model. Environmental Science & Technology, 2016, 50, 8788-8798.	10.0	30
94	In situ high-resolution evaluation of labile arsenic and mercury in sediment of a large shallow lake. Science of the Total Environment, 2016, 541, 83-91.	8.0	30
95	Impacts of CuO nanoparticles on nitrogen removal in sequencing batch biofilm reactors after short-term and long-term exposure and the functions of natural organic matter. Environmental Science and Pollution Research, 2016, 23, 22116-22125.	5.3	29
96	Interpretation of the disparity in harvesting efficiency of different types of Microcystis aeruginosa using polyethylenimine (PEI)-coated magnetic nanoparticles. Algal Research, 2018, 29, 257-265.	4.6	29
97	A BiOBr/Co–Ni layered double hydroxide nanocomposite with excellent adsorption and photocatalytic properties. RSC Advances, 2015, 5, 54613-54621.	3.6	28
98	Intimately coupled photocatalysis and biodegradation for effective simultaneous removal of sulfamethoxazole and COD from synthetic domestic wastewater. Journal of Hazardous Materials, 2022, 423, 127063.	12.4	28
99	Rice-crayfish systems are not a panacea for sustaining cleaner food production. Environmental Science and Pollution Research, 2021, 28, 22913-22926.	5.3	28
100	Effects of cerium oxide nanoparticles on the species and distribution of phosphorus in enhanced phosphorus removal sequencing batch biofilm reactor. Bioresource Technology, 2017, 227, 393-397.	9.6	27
101	Heavy metal pollution status and ecological risks of sediments under the influence of water transfers in Taihu Lake, China. Environmental Science and Pollution Research, 2017, 24, 2653-2666.	5.3	27
102	Harvesting freshwater microalgae with natural polymer flocculants. Algal Research, 2021, 57, 102358.	4.6	27
103	In situ, high resolution ZrO-Chelex DGT for the investigation of iron-coupled inactivation of arsenic in sediments by macrozoobenthos bioturbation and hydrodynamic interactions. Science of the Total Environment, 2016, 562, 451-462.	8.0	26
104	Transport and long-term release behavior of polymer-coated silver nanoparticles in saturated quartz sand: The impacts of input concentration, grain size and flow rate. Water Research, 2017, 127, 86-95.	11.3	26
105	Changes in Microcystis aeruginosa cell integrity and variation in microcystin-LR and proteins during Tanfloc flocculation and floc storage. Science of the Total Environment, 2018, 626, 264-273.	8.0	26
106	Effects of silver sulfide nanoparticles on the microbial community structure and biological activity of freshwater biofilms. Environmental Science: Nano, 2018, 5, 2899-2908.	4.3	26
107	Effects of cerium oxide nanoparticles on bacterial growth and behaviors: induction of biofilm formation and stress response. Environmental Science and Pollution Research, 2019, 26, 9293-9304.	5.3	26
108	Removing specific extracellular organic matter from algal bloom water by Tanfloc flocculation: Performance and mechanisms. Separation and Purification Technology, 2019, 212, 65-74.	7.9	26

#	Article	IF	CITATIONS
109	Effects of sediment physicochemical factors and heavy metals on the diversity, structure, and functions of bacterial and fungal communities from a eutrophic river. Environmental Pollution, 2022, 303, 119129.	7.5	26
110	Synthesis, characterization and photocatalytic activity of BiOBr–AC composite photocatalyst. Composites Part B: Engineering, 2014, 59, 96-100.	12.0	25
111	Preparation of graphene oxide-loaded Ag3PO4@AgCl and its photocatalytic degradation of methylene blue and O2 evolution activity under visible light irradiation. International Journal of Hydrogen Energy, 2015, 40, 1016-1025.	7.1	25
112	ZnO nanorod arrays co-loaded with Au nanoparticles and reduced graphene oxide: Synthesis, characterization and photocatalytic application. Colloids and Surfaces A: Physicochemical and Engineering Aspects, 2016, 492, 71-78.	4.7	25
113	Long-term effects of CuO nanoparticles on the surface physicochemical properties of biofilms in a sequencing batch biofilm reactor. Applied Microbiology and Biotechnology, 2016, 100, 9629-9639.	3.6	24
114	Effects of carbon nanotubes on physicochemical properties and sulfamethoxazole adsorption of sediments with or without aging processes. Chemical Engineering Journal, 2017, 310, 317-327.	12.7	24
115	Effects of pH and natural organic matter (NOM) on the adsorptive removal of CuO nanoparticles by periphyton. Environmental Science and Pollution Research, 2015, 22, 7696-7704.	5.3	23
116	Influence of silver nanoparticles on benthic oxygen consumption of microbial communities in freshwater sediments determined by microelectrodes. Environmental Pollution, 2017, 224, 771-778.	7.5	23
117	Impact of macrozoobenthic bioturbation and wind fluctuation interactions on net methylmercury in freshwater lakes. Water Research, 2017, 124, 320-330.	11.3	23
118	Towards a better understanding on aggregation behavior of CeO2 nanoparticles in different natural waters under flow disturbance. Journal of Hazardous Materials, 2018, 343, 235-244.	12.4	23
119	Influence of extracellular polymeric substances on cell-NPs heteroaggregation process and toxicity of cerium dioxide NPs to Microcystis aeruginosa. Environmental Pollution, 2018, 242, 1206-1216.	7.5	23
120	Attenuation effects of iron on dissemination of antibiotic resistance genes in anaerobic bioreactor: Evolution of quorum sensing, quorum quenching and dynamics of community composition. Journal of Hazardous Materials, 2021, 416, 126136.	12.4	23
121	Preparation of a magnetic graphene oxide–Ag3PO4 composite photocatalyst with enhanced photocatalytic activity under visible light irradiation. Journal of the Taiwan Institute of Chemical Engineers, 2014, 45, 1080-1086.	5.3	21
122	The Fate of p-Nitrophenol in Goethite-Rich and Sulfide-Containing Dynamic Anoxic/Oxic Environments. Environmental Science & Technology, 2020, 54, 9427-9436.	10.0	21
123	Investigation on the adsorption of antibiotics from water by metal loaded sewage sludge biochar. Water Science and Technology, 2021, 83, 739-750.	2.5	21
124	Influence of CeO 2 NPs on biological phosphorus removal and bacterial community shifts in a sequencing batch biofilm reactor with the differential effects of molecular oxygen. Environmental Research, 2016, 151, 21-29.	7.5	20
125	Long term effects of cerium dioxide nanoparticles on the nitrogen removal, micro-environment and community dynamics of a sequencing batch biofilm reactor. Bioresource Technology, 2017, 245, 573-580.	9.6	20
126	Comparison of adsorption behavior studies of methylene blue by microalga residue and its biochars produced at different pyrolytic temperatures. Environmental Science and Pollution Research, 2021, 28, 14028-14040.	5.3	20

#	Article	IF	CITATIONS
127	Polystyrene nanoplastics change the functional traits of biofilm communities in freshwater environment revealed by GeoChip 5.0. Journal of Hazardous Materials, 2022, 423, 127117.	12.4	20
128	Investigation on Ce-doped TiO2-coated BDD composite electrode with high photoelectrocatalytic activity under visible light irradiation. Electrochemistry Communications, 2011, 13, 1423-1423.	4.7	19
129	Optimization of cyanobacterial harvesting and extracellular organic matter removal utilizing magnetic nanoparticles and response surface methodology: A comparative study. Algal Research, 2020, 45, 101756.	4.6	19
130	Nutrient accumulation from excessive nutrient surplus caused by shifting from rice monoculture to rice–crayfish rotation. Environmental Pollution, 2021, 271, 116367.	7.5	19
131	Biofilm influenced metal accumulation onto plastic debris in different freshwaters. Environmental Pollution, 2021, 285, 117646.	7.5	19
132	Preparation and enhanced photocatalytic performance of Sn ion modified titania hollow spheres. Materials Letters, 2011, 65, 3278-3280.	2.6	18
133	Influence of shear forces on the aggregation and sedimentation behavior of cerium dioxide (CeO2) nanoparticles under different hydrochemical conditions. Journal of Nanoparticle Research, 2016, 18, 1.	1.9	18
134	Spatial and Temporal Distribution of Particulate Phosphorus and Their Correlation with Environmental Factors in a Shallow Eutrophic Chinese Lake (Lake Taihu). International Journal of Environmental Research and Public Health, 2018, 15, 2355.	2.6	18
135	Chronic exposure to CuO nanoparticles induced community structure shift and a delay inhibition of microbial functions in multi-species biofilms. Journal of Cleaner Production, 2020, 262, 121353.	9.3	18
136	Simultaneous Removal of Selenite and Selenate by Nanosized Zerovalent Iron in Anoxic Systems: The Overlooked Role of Selenite. Environmental Science & Technology, 2021, 55, 6299-6308.	10.0	18
137	The performance of chitosan/montmorillonite nanocomposite during the flocculation and floc storage processes of Microcystis aeruginosa cells. Environmental Science and Pollution Research, 2015, 22, 11148-11161.	5.3	17
138	A novel co-graft tannin-based flocculant for the mitigation of harmful algal blooms (HABs): The effect of charge density and molecular weight. Science of the Total Environment, 2022, 806, 150518.	8.0	17
139	A critical review on the interaction of iron-based nanoparticles with blue-green algae and their metabolites: From mechanisms to applications. Algal Research, 2022, 64, 102670.	4.6	17
140	Nitrogen Distribution and Potential Mobility in Sediments of Three Typical Shallow Urban Lakes in China. Environmental Engineering Science, 2009, 26, 1511-1521.	1.6	16
141	Insights into spatial effects of ceria nanoparticles on oxygen mass transfer in wastewater biofilms: Interfacial microstructure, in-situ microbial activity and metabolism regulation mechanism. Water Research, 2020, 176, 115731.	11.3	16
142	Antibiotic resistance genes alternation in soils modified with neutral and alkaline salts: interplay of salinity stress and response strategies of microbes. Science of the Total Environment, 2022, 809, 152246.	8.0	16
143	Preparation of graphene-modified TiO2 nanorod arrays with enhanced photocatalytic activity by a solvothermal method. Materials Letters, 2013, 101, 41-43.	2.6	15
144	Process Optimization for Microcystin-LR Adsorption onto Nano-sized Montmorillonite K10: Application of Response Surface Methodology. Water, Air, and Soil Pollution, 2014, 225, 1.	2.4	15

#	Article	IF	CITATIONS
145	Strategies and relative mechanisms to attenuate the bioaccumulation and biotoxicity of ceria nanoparticles in wastewater biofilms. Bioresource Technology, 2018, 265, 102-109.	9.6	15
146	Periphytic Biofilm Formation on Natural and Artificial Substrates: Comparison of Microbial Compositions, Interactions, and Functions. Frontiers in Microbiology, 2021, 12, 684903.	3.5	15
147	Photocatalytic performance of Gd ion modified titania porous hollow spheres under visible light. Materials Letters, 2010, 64, 1003-1006.	2.6	14
148	Enhanced anaerobic biological treatment of chlorpyrifos in farmland drainage with zero valent iron. Chemical Engineering Journal, 2018, 336, 352-360.	12.7	14
149	The effects of extracellular polymeric substances on magnetic iron oxide nanoparticles stability and the removal of microcystin-LR in aqueous environments. Ecotoxicology and Environmental Safety, 2018, 148, 89-96.	6.0	14
150	Influence of aggregation and sedimentation behavior of bare and modified zero-valent-iron nanoparticles on the Cr(VI) removal under various groundwater chemistry conditions. Chemosphere, 2022, 296, 133905.	8.2	13
151	Seasonal, Spatial Distribution and Ecological Risk Assessment of Heavy Metals in Surface Sediments from a Watershed Area in Gonghu Bay in Taihu Lake, China. Terrestrial, Atmospheric and Oceanic Sciences, 2014, 25, 605.	0.6	12
152	Mechanistic understanding of cerium oxide nanoparticle-mediated biofilm formation in Pseudomonas aeruginosa. Environmental Science and Pollution Research, 2018, 25, 34765-34776.	5.3	11
153	Development of a comprehensive understanding of aggregation-settling movement of CeO2 nanoparticles in natural waters. Environmental Pollution, 2020, 257, 113584.	7.5	11
154	Early diagenetic alterations of biogenic and reactive silica in the surface sediment of the Yangtze Estuary. Continental Shelf Research, 2015, 99, 1-11.	1.8	10
155	Zr oxide-based coloration technique for two-dimensional imaging of labile Cr(VI) using diffusive gradients in thin films. Science of the Total Environment, 2016, 566-567, 1632-1639.	8.0	10
156	Preparation of heterostructured Ag@AgCl/La ₂ Ti ₂ O ₇ plasmonic photocatalysts with high visible light photocatalytic performance for the degradation of organic pollutants. RSC Advances, 2016, 6, 19223-19232.	3.6	10
157	Quantitative measurement of aggregation kinetics process of nanoparticles using nanoparticle tracking analysis and dynamic light scattering. Journal of Nanoparticle Research, 2019, 21, 1.	1.9	10
158	Flow characteristics of the wind-driven current with submerged and emergent flexible vegetations in shallow lakes. Journal of Hydrodynamics, 2016, 28, 746-756.	3.2	9
159	Surface Properties and Environmental Transformations Controlling the Bioaccumulation and Toxicity of Cerium Oxide Nanoparticles: A Critical Review. Reviews of Environmental Contamination and Toxicology, 2020, 253, 155-206.	1.3	9
160	Deciphering the effects of CeO2 nanoparticles on Escherichia coli in the presence of ferrous and sulfide ions: Physicochemical transformation-induced toxicity and detoxification mechanisms. Journal of Hazardous Materials, 2021, 413, 125300.	12.4	9
161	One-pot synthesis of AgBr/Ag2CO3 heterojunctions with enhanced visible-light photocatalytic activity. Materials Letters, 2016, 163, 258-261.	2.6	8
162	Dynamic responses of community structure and microbial functions of periphytic biofilms during chronic exposure to TiO ₂ NPs. Environmental Science: Nano, 2020, 7, 665-675.	4.3	8

#	Article	IF	CITATIONS
163	Biochar produced from the co-pyrolysis of sewage sludge and waste tires for cadmium and tetracycline adsorption from water. Water Science and Technology, 2021, 83, 1429-1445.	2.5	8
164	Effects of titanium dioxide (TiO 2) nanoparticles on the photodissolution of particulate organic matter: Insights from fluorescence spectroscopy and environmental implications. Environmental Pollution, 2017, 229, 19-28.	7.5	8
165	Response surface modeling and optimization of microcystin-LR removal from aqueous phase by polyacrylamide/sodium alginate–montmorillonite superabsorbent nanocomposite. Desalination and Water Treatment, 2015, 56, 1121-1139.	1.0	7
166	Influence of CeO2 nanoparticles on viscoelastic properties of sludge: Role of extracellular polymeric substances. Environmental Research, 2018, 167, 34-41.	7.5	7
167	lodideâ€Induced Fragmentation of Polymerized Hydrophilic Carbon Nitride for High Performance Quasiâ€Homogeneous Photocatalytic H2O2 Production. Angewandte Chemie, 0, , .	2.0	7
168	Microbial Carbon Metabolic Functions in Sediments Influenced by Resuspension Event. Water (Switzerland), 2021, 13, 7.	2.7	7
169	The Evaluation on the Cadmium Net Concentration for Soil Ecosystems. International Journal of Environmental Research and Public Health, 2017, 14, 297.	2.6	6
170	In situ prepared algae-supported iron sulfide to remove hexavalent chromium. Environmental Pollution, 2021, 274, 115831.	7.5	6
171	Exposure-Dose-Response Relationships of the Freshwater Bivalve <i>Corbicula fluminea</i> to Inorganic Mercury in Sediments. Journal of Computational and Theoretical Nanoscience, 2016, 13, 5714-5723.	0.4	6
172	The role of nitrate in simultaneous removal of nitrate and trichloroethylene by sulfidated zero-valent Iron. Science of the Total Environment, 2022, 829, 154304.	8.0	6
173	A innovative stepwise strategy using magnetic Fe3O4-co-graft tannin/polyethyleneimine composites in a coupled process of sulfate radical-advanced oxidation processes to control harmful algal blooms. Journal of Hazardous Materials, 2022, 439, 129485.	12.4	6
174	Seasonal and spatial variations of acid-volatile sulphide and simultaneously extracted metals in the Yangtze River Estuary. Chemistry and Ecology, 2015, 31, 466-477.	1.6	5
175	Comparison of in situ DGT measurement with ex situ methods for predicting cadmium bioavailability in soils with combined pollution to biotas. Water Science and Technology, 2017, 75, 2171-2178.	2.5	5
176	Climatological characteristics of frontogenesis and related circulations over East China in June and July. Journal of Meteorological Research, 2013, 27, 144-169.	1.0	4
177	Nutrient Speciation and Distribution between Surface Water and Sediment in the Middle Reach of the Huai River, China. Journal of Environmental Engineering, ASCE, 2013, 139, 226-234.	1.4	4
178	Presence and patterns of alkaline phosphatase activity and phosphorus cycling in natural riparian zones under changing nutrient conditions. Journal of Limnology, 2014, 73, .	1.1	4
179	Investigation of the rheological behavior of activated sludge in response to CeO2 nanoparticles and potential mechanism. Environmental Science and Pollution Research, 2018, 25, 29725-29733.	5.3	3
180	Synergistic effect of surface phase junction and surface defects on enhancing the photocatalytic performance of BiPO ₄ . Micro and Nano Letters, 2018, 13, 720-724.	1.3	3

#	Article	IF	CITATIONS
181	Optimized ratoon rice system to sustain cleaner food production in Jianghan Plain, China: a comprehensive emergy assessment. Environmental Science and Pollution Research, 2021, , 1.	5.3	3
182	Contributions of different fractions of extracellular polymeric substances from waste-activated sludge to Cu(II) biosorption. Desalination and Water Treatment, 2016, 57, 21405-21416.	1.0	2
183	Speciation of potentially mobile Si in Yangtze Estuary surface sediments: estimates using a modified sequential extraction technique. Environmental Science and Pollution Research, 2016, 23, 18928-18941.	5.3	2
184	Keystone indices probabilistic species sensitivity distribution in the case of the derivation of water quality criteria for copper in Tai Lake. Environmental Science and Pollution Research, 2016, 23, 13047-13061.	5.3	2
185	Can the carbon metabolic activity of biofilm be regulated by the hydrodynamic conditions in urban rivers?. Science of the Total Environment, 2022, 832, 155082.	8.0	2
186	Insights into the Characteristics, Adsorption, and Desorption Behaviors of Polylactic Acid Aged with or without Salinities. Journal of Environmental Engineering, ASCE, 2022, 148, .	1.4	2
187	Neutral network compensator based cascade control for ball and beam system. , 2010, , .		1
188	Purifying Effects of Nitrogen in Wangyu River Water through Natural Wetlands. Advanced Materials Research, 2013, 664, 87-93.	0.3	1
189	DEVELOPMENT OF A MULTI-INDEX ECOSYSTEM HEALTH ASSESSMENT MODEL USING BACK-PROPAGATION NEURAL NETWORK APPROACH: A CASE STUDY OF THE YANGTZE ESTUARY, CHINA. Environmental Engineering and Management Journal, 2017, 16, 1551-1561.	0.6	1
190	Notice of Retraction: Effects of Cd on the Chlorophyll, Dry Weight and Nutrient Element Uptake of Chinese Cabbage. , 2011, , .		0
191	Application of fuzzy mathematics in health assessment of estuarine ecosystem. , 2011, , .		0